Cyclotron Resonance in Magnesium*

D. A. Zych† and T. G. Eck
Department of Physics, Case Western Reserve University, Cleveland, Ohio 44106
(Received 11 September 1969)

Azbel'-Kaner cyclotron resonance has been studied at 22.9 GHz and 2 °K in the $\{10\bar{1}0\}$, $\{11\bar{2}0\}$, $\{0001\}$, and $\{10\bar{1}1\}$ planes of magnesium. Fifteen distinct mass series have been identified and their mass values determined as a function of the orientation of the magnetic field in the sample surface. Nearly all of the observed signals have been successfully assigned to the Fermi surface of Mg determined by Stark and his co-workers. Our results are in excellent agreement with their magnetoacoustic and de Haas–van Alphen measurements and their pseudopotential band-structure calculation *except* for the absence of cyclotron resonance signals from the "giant" orbit and the hexagonal grid of coupled orbits so prominent in the de Haas–van Alphen data. The absence of cyclotron resonance signals from these orbits confirms Moore's conclusion that cyclotron resonance signals will not be seen from orbits in the intermediate stage of magnetic breakdown.

I. INTRODUCTION

The Fermi surface (FS) of magnesium has been studied extensively, both experimentally and theoretically. Most recently Stark and his co-workers have calipered the FS using magnetoacoustic attenuation,[1] determined extremal cross-sectional areas on all pieces of the FS using the de Haas–van Alphen (DHVA) technique,[2] and performed a pseudopotential band-structure calculation[3] to obtain a model for the FS which is in very good agreement with their experimental data. The reader is referred to the first of these papers for an extensive bibliography of previous work on the FS of Mg.

In this paper we present the results of our cyclotron resonance (CR) investigation of magnesium. The only previous CR data for Mg were obtained in a preliminary investigation in our laboratory,[4] though Stark[2] has determined cyclotron masses for several selected orbits on the FS from the temperature dependence of the amplitude of his DHVA oscillations.

II. THEORY

In two previous publications[5,6] we have reported on our CR investigations of zinc and cadmium. A summary of the theory of CR most pertinent to the interpretation of experimental data is given in Sec. II of Ref. 5. Here we present a brief recapitulation of that discussion and consider additional points necessary for the interpretation of our Mg data.

In an Azbel'-Kaner CR experiment, where the magnetic field $\vec{H}$ is aligned precisely parallel to a smooth plane surface of the metal under investigation, resonances in the surface impedance occur when $\omega = n\omega_c = neH/m^*c$, where ω is the angular frequency of the incident electromagnetic radiation, n is an integer, m^* is the cyclotron effective mass of the orbiting charge carrier, e is the magnitude of the charge on the electron, and c is the speed of light, which appears because of our choice of Gaussian units. It is most common to hold ω fixed, vary the magnetic field strength H, and observe dR/dH, the field derivative of the resistive part of the surface impedance. The CR signal then appears as a subharmonic series of resonances, and m^* can be determined from the slope of a plot of $1/H_n$ versus n, where H_n is the field strength corresponding to the dR/dH maximum of the nth subharmonic resonance.

The observed resonances arise from electrons on regions of the FS for which $\partial m^*/\partial k_H = 0$, where k_H is the component parallel to $\vec{H}$ of the charge-carrier's wave vector $\vec{k}$. Chambers[7] has obtained theoretical expressions for the variation of dR/dH with H near resonance for m^* versus k_H a local minimum, m^* a local maximum, and m^* constant with varying k_H. These theoretical resonance line shapes are in good qualitative agreement with those observed experimentally.[6] Thus, we can use the observed line shape as an aid in identifying the orbit on the FS responsible for a particular resonance series. Another aid in identifying the region of the FS responsible for given CR series is the effect of the relative orientation of $\vec{H}$ and $\vec{E}_{rf}$, the oscillating electric field at the surface, on the strength of the resonance signal. The strength of the resonance is proportional to the component of $\vec{E}_{rf}$ parallel to the velocity of the charge carrier when it is in the skin depth. Thus, carriers that pass through the skin depth with their velocities perpendicular to $\vec{H}$ will give the largest signal for $\vec{E}_{rf}$ perpendicular to $\vec{H}$ and no signal for $\vec{E}_{rf}$ parallel to $\vec{H}$. Also important for the identification of a resonance is the investigation of its "tilt sensitivity," the effect on

the strength of the signal of tilting $\vec{H}$ from the sample surface. Resonances from carriers on orbits for which v_d, the net drift velocity parallel to $\vec{H}$, is zero are relatively unaffected when $\vec{H}$ is tilted slightly from the surface, while resonances from orbits with $v_d \neq 0$ are strongly attenuated for tilts as small as a few minutes of arc. The signals seen in a DHVA experiment arise from carriers with $v_d = 0$, since extremal area, the criterion for the observation of a DHVA signal, implies a vanishing net drift velocity.[8] The $\partial m^*/\partial k_H = 0$ orbit responsible for a CR signal may or may not have $v_d = 0$.

The magnetoacoustic data of Ketterson and Stark[1] show that the FS of Mg is quite free-electron-like with only slight rounding of the sharp edges predicted by the single-orthogonalized-plane-wave (single-OPW) model for the FS. For such a surface the strength of the CR signals with $\vec{H}$ in a given crystallographic direction can depend quite strongly on which crystal plane is exposed to the microwave radiation. Thus, if the portion of the electron's real-space orbit which lies in the skin depth corresponds to a sharp edge of the orbit in $\vec{k}$ space, the interaction with $\vec{E}_{rf}$ will be weak and the CR signal small. Spong and Kip[9] observed this phenomenon in their investigation of the sharply cusped hole surface in the second band of aluminum. Our CR data confirm that the FS of Mg has the sharp edges deduced from the magnetoacoustic results. An especially striking example is provided by the data for the lens-shaped electron surface in the third band of Mg. The signal from the central orbit on this surface was the strongest observed in all of our data when $\vec{H}$ was perpendicular to $\langle 0001 \rangle$ *and* the sample surface exposed to the microwave radiation was either a $\{10\bar{1}0\}$ or $\{11\bar{2}0\}$ plane. With a $\{0001\}$ surface the lens signal was below the noise level. Actually, the absence of a strong signal from the lens in the $\{0001\}$ plane data was fortunate, since its subharmonics would have obscured and distorted signals from other parts of the FS which were seen clearly in the $\{0001\}$-plane data.

Moore[10] has discussed the strength of CR signals in the presence of magnetic breakdown and concludes that for the observation of a CR signal the probability of the electron "tunneling" from one sheet of the FS to another must be very close to either zero or one. This rules out the observation of "compound" orbits involving breakdown at some points and Bragg reflection at other (equivalent) points on the orbit. Stark's Mg DHVA data for $\vec{H}$ near $\langle 0001 \rangle$ are dominated by signals arising from magnetic breakdown between the second-band hole surface and a piece of electron surface in the third band, the "cigar." Figure 13 of Ref. 2 shows some of the many possible orbits which one can construct by considering various combinations of tunneling and Bragg reflection at successive encounters of the electron with the small energy gap between the second-band surface and the cigar. In agreement with Moore's prediction, we have seen no evidence in our CR data of signals from these compound orbits.

III. EXPERIMENTAL DETAILS

The Mg crystals used for this investigation were grown directly from the vapor phase in a high-vacuum gradient furnace, a technique developed by Stark.[11] With this technique, the $\{0001\}$, $\{10\bar{1}0\}$, and $\{10\bar{1}1\}$ planes of Mg occur as natural growth surface planes which can be used for CR measurements without further preparation. These crystals were cut to the proper size for mounting with an acid string saw while the natural faces were protected from the acid fumes by a coating of Apiegon N grease. This coating did not strain the surface and was easily removed with benzene. The $\{11\bar{2}0\}$ surfaces were prepared by cutting with an acid string saw crystals oriented to within $\frac{1}{2}$ deg using standard x-ray techniques. These surfaces were then lapped and electropolished.[12] Eight different specimens were investigated, two each with surfaces parallel to $\{11\bar{2}0\}$, $\{10\bar{1}0\}$, $\{10\bar{1}1\}$, and $\{0001\}$.

We attempted to determine the residual resistance ratio ($\rho_{300\,^\circ K}/\rho_{4.2\,^\circ K}$) of our sublimed Mg from dc resistance measurements in zero magnetic field on samples cut with an acid string saw, but found that for samples of small cross section the low-temperature resistance was size-effect limited, and for samples of large cross section the voltage across the sample for reasonable currents was near the noise level of our voltmeter. Extrapolation of resistance measurements made in small transverse magnetic fields gave a value for the zero-field bulk-residual-resistance ratio of at least 100 000. A transverse magnetic field of 10 kG increased the resistance at 4.2 °K to almost three times the resistance at room temperature.

The specimen surfaces were exposed to 22.9-GHz electromagnetic radiation by making them one of the end walls of a TE_{111} cylindrical cavity. This resonant cavity was similar in design to one developed by Koch *et al.*[13,9] and allows one to align $\vec{H}$ accurately parallel to the specimen surface, to orient $\vec{E}_{rf}$ either parallel or perpendicular to $\vec{H}$, and to align any crystallographic direction in the sample surface parallel to $\vec{H}$. Further details of the cavity, specimen mounting, microwave system, and signal detection are given in

Sec. III of Ref. 5. It was necessary for the present investigation to modify the resonant cavity used for our Zn and Cd measurements since the largest Mg natural growth surfaces we succeeded in growing were not large enough to fully cover the 0.380-in.-diam cavity. New cavities were machined with a tapered end wall to reduce the area of the specimen surface exposed to the microwave radiation. The angle of taper was nominally 5 deg and cavities were made with openings ranging from $\frac{1}{8}$ to $\frac{1}{4}$ in. in diam. The presence of this taper reduced somewhat the cavity Q. However, after silver plating and polishing, the Q's at 2 °K were still near 5000.

The flatness of the speciman surfaces was estimated from the angle through which $\vec{H}$ could be tilted from the surface without causing a noticeable effect (decrease in signal strength or shift in position of resonance) on the CR signals. The natural growth surfaces were flat to approximately $\frac{2}{100}$ of a degree of arc over the area exposed to the microwaves, while the $\{11\bar{2}0\}$ surfaces had a residual rounding or waviness almost 10 times this value. The angle between $\vec{H}$ and the surface could be set reproducibly to within $\frac{1}{100}$ of a degree.

To obtain an order-of-magnitude estimate of $\omega\tau$, where τ is the resonating charge-carrier's relaxation time, we compared the width of one of the CR signals with a line shape corresponding to m^* versus k_H a local minimum with that predicted by Chambers's analysis.[7] This comparison gave $\omega\tau \cong 75$, which should be considered a lower limit since any rounding or strain of the specimen surface tends to broaden the resonance line and decrease the apparent $\omega\tau$. This value of $\omega\tau$ is in the range for which Chambers's lineshape analysis is valid. A detailed investigation of relaxation times and magnetic field tilt effects for some of the CR signals observed in Mg is underway.[14]

As discussed in Sec. II, the value of m^* for a particular subharmonic series of resonances is determined from the periodicity in $1/H$ of the dR/dH maxima of this series. The precision of the cyclotron mass determined from a given resonance series is limited by the shift of the field positions of the dR/dH maxima for finite $\omega\tau$ (see Ref. 7), the effects of curvature of the specimen surface, and the precision with which the H values of the dR/dH maxima can be determined from the recorder traces. For strong signals which are well resolved from overlapping resonances and are not tilt sensitive the uncertainty in m^* is set by the first of these effects and is of the order of 1% for an $\omega\tau$ of 75. One can correct for the shift of the dR/dH maxima introduced by the finite $\omega\tau$ by determining $\omega\tau$ from the signal width and correcting m^* as indicated by Chambers's analysis. However, since such a correction is of questionable validity unless there is detailed agreement between the theoretical and experimental line shapes, we assign a minimum uncertainty of about 1% to our measured masses.

IV. CYCLOTRON MASSES AND ORBIT ASSIGNMENTS

Since the pseudopotential band-structure calculation of Ref. 3 yields an Fs for Mg (Figs. 7 and 8 of Ref. 3) which closely resembles that of the single-OPW model, we shall base our discussion of the CR data on the single-OPW FS, indicating any modifications which are necessary to accommodate our results. Figure 1, taken from Ref. 1, shows the single-OPW FS for Mg. The Greek letters in Fig. 1(a) indicate orbits on this sheet of the FS which are referred to in the following discussion of the CR data. The reader is referred to Ref. 1 for detailed descriptions of the various sheets of the single-OPW FS for Mg.

Figure 2 shows the values obtained for m^*/m_0 as a function of the orientation of $\vec{H}$ parallel to the specimen surface in the three principal crystal planes. m_0 is the mass of the free electron. We have not shown a plot of m^*/m_0 for the $\{10\bar{1}1\}$ plane since it serves only to confirm the data of Fig. 2. The uncertainty in the angular position of any data point is no greater than $\frac{5}{8}$ of a degree, the accuracy to which the orientation of the crystal could be reset with respect to the direction of $\vec{H}$. When a given resonance series could be ob-

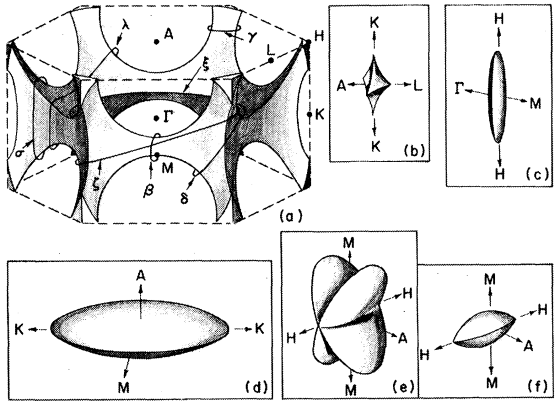

FIG. 1. Single-OPW FS for magnesium: (a) monster (second-band holes); (b) cap (first-band holes); (c) cigar (third-band electrons); (d) lens (third-band electrons); (e) butterfly (third-band electrons); (f) fourth-band electron pockets. Capital letters designate symmetry points of the Brillouin zone and small Greek letters indicate orbits on the monster which are referred to in text.

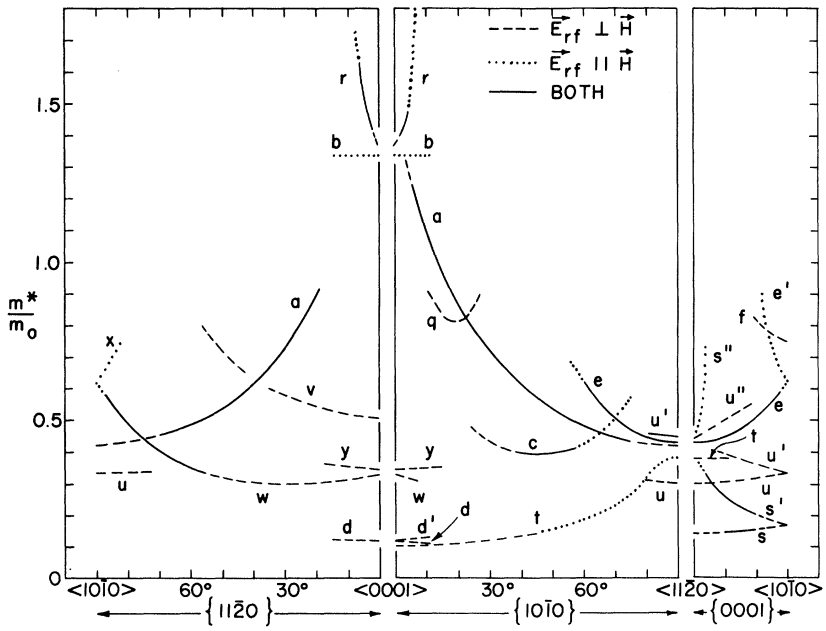

FIG. 2. Cyclotron effective masses in Mg as a function of the orientation of the magnetic field parallel to the specimen surface in the three principal crystal planes.

served with $\vec{E}_{rf}$ both perpendicular and parallel to $\vec{H}$, there was no significant disagreement between the two mass values obtained. Table I lists the cyclotron masses for signals observed in symmetry directions. The uncertainty assigned to each of the CR mass values in Table I is our 80% confidence limit.

The mass plot consists basically of 15 branches labeled a through f and q through y. Branches labeled with a primed or double-primed letter have been assigned to orbits on the FS which are related in an obvious manner by crystal symmetry to the orbit responsible for the branch designated by the unprimed letter. Branches a through f have their counterpart in the a through f branches of the Zn and Cd mass plots.[5,6] With one exception, discussed below, no signals have been seen in Mg which correspond to the g through p branches of the Zn and Cd data.

In the remainder of this section we shall consider in turn each sheet of the FS, assigning the branches of the mass plot to orbits on these various

TABLE I. CR and DHVA masses in symmetry directions.

Branch	Orbit	Magnetic field directions	m^*/m_0(CR)	m^*/m_0(DHVA)[a]
a	Lens central	$\langle 10\bar{1}0\rangle$	0.421 ± 0.009	0.42 ± 0.01
		$\langle 11\bar{2}0\rangle$	0.420 ± 0.004	0.42 ± 0.01
b	Limiting point	$\langle 0001\rangle$	1.335 ± 0.010	
d	γ	$\langle 0001\rangle$	0.114 ± 0.003	0.11 ± 0.01
e	σ	$\langle 10\bar{1}0\rangle$	0.625 ± 0.020	
		$\langle 11\bar{2}0\rangle$	0.431 ± 0.004	0.45 ± 0.03
f	λ	$\langle 10\bar{1}0\rangle$	0.754 ± 0.010	
r	ξ	$\langle 0001\rangle$	1.370 ± 0.020	
s	β	$\langle 10\bar{1}0\rangle$	0.166 ± 0.004	0.162 ± 0.004
		$\langle 11\bar{2}0\rangle$	0.140 ± 0.004	0.138 ± 0.004
t	Cigar	$\langle 11\bar{2}0\rangle$	0.381 ± 0.008	0.38 ± 0.03
		$\langle 0001\rangle$	0.103 ± 0.002	0.100 ± 0.002
u	Clam	$\langle 10\bar{1}0\rangle$	0.334 ± 0.007	
		$\langle 11\bar{2}0\rangle$	0.302 ± 0.006	0.32 ± 0.01
u'	Clam	$\langle 11\bar{2}0\rangle$	0.446 ± 0.005	
v	Clam	$\langle 0001\rangle$	0.507 ± 0.008	0.49 ± 0.02
w	Fourth band	$\langle 10\bar{1}0\rangle$	0.615 ± 0.010	
	Electron pocket	$\langle 0001\rangle$	0.329 ± 0.008	0.34 ± 0.02
x	Butterfly	$\langle 10\bar{1}0\rangle$	0.615 ± 0.010	
y	Breakdown	$\langle 0001\rangle$	0.346 ± 0.006	0.340 ± 0.005

[a]Taken from Table I of Ref. 2.

sheets and considering the consistency of these assignments with the results of Refs. 1–3.

A. First-Band Cap

None of the CR signals have been assigned to the first-band cap [Fig. 1(b)]. Stark has seen a weak DHVA signal attributed to the central orbit around the cap for $\vec{H}$ within 6° of ⟨0001⟩ and for field strengths less than 3.1 kG. As $\vec{H}$ was tilted from ⟨0001⟩, this signal vanished because of magnetic breakdown of the small spin-orbit energy gap which separates the cap from the second-band hole surface. It is not too surprising that we have been unable to find a small cap signal for $\vec{H}$ near ⟨0001⟩ since such a signal would be obscured by the signals from branches d, t, and w.

B. Second-Band Monster

Seven of the 15 branches of the mass plot are assigned to this sheet of the FS. They are branches c, d, e, f, and q, r, s.

Branch c is assigned to an orbit about the intersection of two diagonal arms of the monster with the monster waist, the δ orbit of Fig. 1(a). The signals from branch c fell below the noise level for $\vec{H}$ 24° from ⟨0001⟩ and 15° from ⟨11$\bar{2}$0⟩. These angles do not correspond to sharp cutoffs and, hence, cannot be associated with any dimension of the monster. The line shape of c, shown in Fig. 3, corresponds to m^* versus k_H a local minimum, which is consistent with its assignment to the δ orbit. The c signal is moderately tilt sensitive indicating that it comes from a "nonstationary" orbit ($v_d \neq 0$). We have not seen signals from a δ orbit in specimens with a {11$\bar{2}$0} surface. This is surprising, even given the greater curvature of our {11$\bar{2}$0} surfaces, since for $\vec{H}$ parallel to a {11$\bar{2}$0} plane the δ orbit must be stationary by crystal symmetry. The explanation is provided by Stark's DHVA data. His μ_2^5 orbit, which is identical to a {11$\bar{2}$0}-plane δ orbit, is coupled by magnetic breakdown to the cigar as evidenced by the presence of the D_2^1 branch in his area plot. The presence of both μ_2^5 and D_2^1 signals in the DHVA data shows that this breakdown is not complete. Therefore, as discussed in Sec. II, we would not expect to see CR signals from either of these orbits. Since Stark also sees a δ-type orbit (μ_1^6) and a breakdown orbit (D_1^1) in the {10$\bar{1}$0} plane, one may well wonder why we see CR signals from a δ orbit in this plane. Here, however, crystal symmetry does not require that the δ orbit of extremal m^* coincide with that of extremal area. In fact, the tilt sensitivity of the c signal indicates that they are not the same orbit. Furthermore, Stark concludes from the analysis of his measured areas that his μ_1^6 and D_1^1 orbits do not lie in quite the same plane.

Branch d is assigned to an orbit around the diagonal arm of the monster, the γ orbit of Fig. 1(a). The d signal has the expected minimum m^* line shape and is not tilt sensitive, indicating that the CR γ orbit coincides with or is near to the corresponding DHVA orbit. As $\vec{H}$ is tilted from ⟨0001⟩ in the {10$\bar{1}$0} plane d should split into four subbranches corresponding to Stark's μ_1^1, μ_1^2, μ_1^3, and μ_1^4. We have seen only two subbranches, d and d' of Fig. 2. For $\vec{H}$ tilted from ⟨0001⟩ in the {11$\bar{2}$0} plane there should be three d subbranches. The one rather broad signal we see in this plane is most likely an unresolved superposition of these three signals. For $\vec{H}$ beyond about 15° from ⟨0001⟩ in either the {10$\bar{1}$0} or {11$\bar{2}$0} plane, the d signal is lost in the strong subharmonics of the signal from branch a. From Table I we see that the CR and DHVA values of m^*/m_0 for $\vec{H}$ parallel to ⟨0001⟩ are in good agreement, though the latter has a rather large uncertainty.

Branch e is assigned to another orbit about the intersection of two diagonal arms of the monster with the monster waist, the σ orbit of Fig. 1(a). The signals from this branch are the strongest of any associated with the monster and reach a maximum strength in both the {10$\bar{1}$0} and {0001} planes when $\vec{H}$ is parallel to ⟨11$\bar{2}$0⟩. Stark's σ-type orbit (μ_1^7 in the {10$\bar{1}$0} plane and μ_3^4 in the {0001} plane)

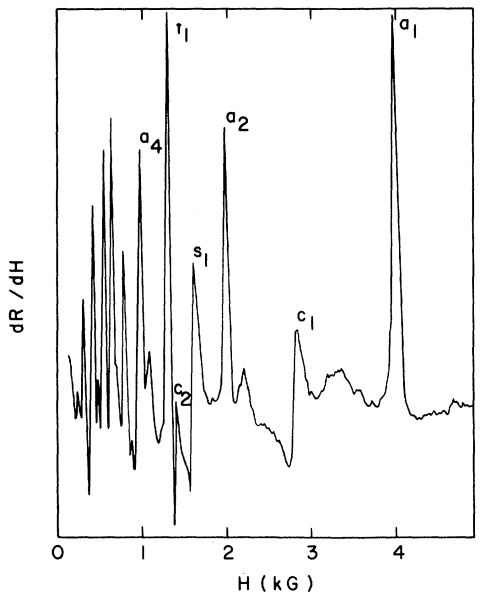

FIG. 3. Cyclotron resonance signals in Mg for $\vec{H}$ 43° from ⟨11$\bar{2}$0⟩ in a {10$\bar{1}$1} surface. $\vec{E}_{rf}$ is perpendicular to $\vec{H}$.

cuts off sharply 18.5° from $\langle 11\bar{2}0\rangle$ in the $\{0001\}$ plane, while our e branch in the $\{0001\}$ plane extends beyond $\langle 10\bar{1}0\rangle$. In fact, the termination of the e' branch does not correspond to a sharp cutoff. Thus, the CR and DHVA σ orbits occur at different values of k_H. This is confirmed by the tilt sensitivity of our e signal indicating that $v_d \neq 0$ for the CR orbit. We attribute the absence of an e signal in the $\{11\bar{2}0\}$ plane to this nonvanishing drift velocity and the greater curvature of our $\{11\bar{2}0\}$ surfaces. The line shape of e for $\vec{H}$ parallel to $\langle 11\bar{2}0\rangle$ is shown in Fig. 4 and suggests a broad minimum in m^* versus k_H. Such a broad minimum would explain the strength of the e signal and also the fact that the values of m^*/m_0 for the extremal mass and extremal area orbits are nearly the same (see Table I) even though these orbits occur at different values of k_H.

Branch f is assigned to a dog's-bone-shaped orbit running along the monster waist and around two intersections of diagonal arms with the waist, the λ orbit of Fig. 1(a). Both the single-OPW and pseudopotential FS models predict that there is no λ-type orbit of extremal area. As one proceeds from the inside of the monster waist to the outside, this orbit increases monotonically in area and then breaks sharply into two orbits. Thus, it is not surprising that the DHVA data show no evidence of a signal from this type of orbit. However, since planes perpendicular to $\vec{H}$ and tangent to the inside and outside of the monster waist intersect the FS in figure-eight orbits for which m^* is infinite (see discussion in Sec. II of Ref. 5), an orbit of minimum m^*, the λ orbit, must exist on this section of the monster. The f signal is very tilt sensitive in agreement with its assignment to a nonstationary orbit. Its line shape, though quite different from Chambers's prediction for a minimum m^*, closely resembles that of the e signal for $\vec{H}$ near $\langle 10\bar{1}0\rangle$. As in the case of the e signal, we attribute the absence of an f signal in our $\{11\bar{2}0\}$-plane data to the greater curvature of our $\{11\bar{2}0\}$ surfaces.

Branch q is assigned to an orbit centered on the ΓM line of the Brillouin zone and passing around two intersections of diagonal arms with the monster waist, the ζ orbit of Fig. 1(a). The q signal has a line shape which is clearly that of a minimum m^* and, in agreement with its assignment to a stationary orbit with reflection symmetry in the ΓM line, is not tilt sensitive. Branch q extends from 11° to 27° from $\langle 0001\rangle$ in the $\{10\bar{1}0\}$ plane. The angle at which the ζ orbit cuts off as $\vec{H}$ approaches $\langle 0001\rangle$ is determined by the minimum height of the monster waist. Our observation of the ζ orbit up to 11° from $\langle 0001\rangle$ is inconsistent with a cutoff angle of 13.3° predicted by the single-OPW model. However, it is well established that the height of the monster waist is substantially less than its single-OPW value.[1,3,15] Our results are quite consistent with the value of Stark *et al.*[15] of 0.20 Å^{-1} for this dimension of the monster. Since the ζ orbit is stationary, it should be observable in a DHVA investigation. As yet, no observation of a DHVA signal from this orbit has been reported.

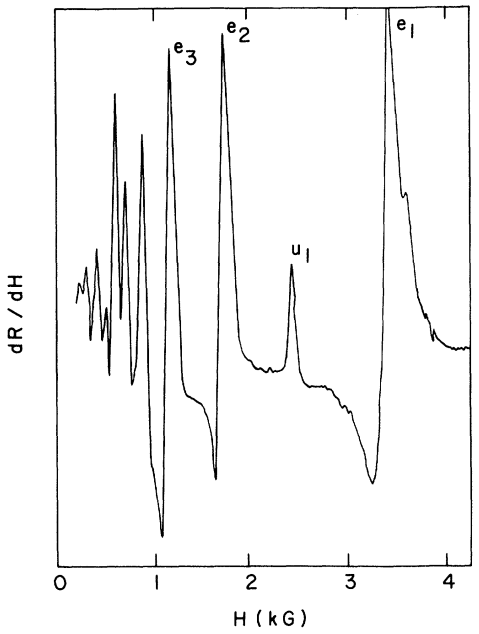

FIG. 4. CR signals in Mg for $\vec{H}$ parallel to $\langle 11\bar{2}0\rangle$ in a $\{0001\}$ surface. $\vec{E}_{rf}$ is perpendicular to $\vec{H}$. Subharmonics of branch u are obscured by the much stronger signal from branch e.

Branch r is assigned to the orbit around the inside of the monster waist, the ξ orbit of Fig. 1(a). The r signal, shown in Fig. 5, has the expected minimum m^* line shape. Also, this signal is not tilt sensitive, in agreement with its assignment to a stationary orbit centered on Γ. As $\vec{H}$ is tilted from $\langle 0001\rangle$, the ξ orbit cuts off at an angle which is determined by the minimum height of the monster waist. The observed cutoff angle of branch r is close to 7° for both the $\{10\bar{1}0\}$ and and $\{11\bar{2}0\}$ planes, in excellent agreement with the value of Stark *et al.*[15] of 0.20 Å^{-1} for the height of the monster waist. Stark has not seen a DHVA signal from the ξ orbit. This is probably because it is obscured by the large number of strong DHVA signals from magnetic breakdown orbits that are present when $\vec{H}$ is near $\langle 0001\rangle$.

An alternative assignment of branch r, which is consistent with its angular range and with the line shape and lack of tilt sensitivity of the r

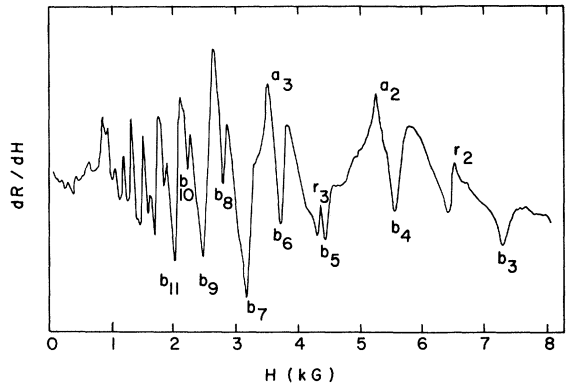

FIG. 5. CR signals in Mg for $\vec{H}$ 5.5° from ⟨0001⟩ in a $\{10\bar{1}0\}$ surface. $\vec{E}_{rf}$ is parallel to $\vec{H}$.

signal, is to the orbit around the *outside* of the monster waist. However, the signal from this orbit should be strongest for $\vec{E}_{rf}$ perpendicular to $\vec{H}$ and should increase in strength as $\vec{H}$ approaches ⟨0001⟩. The r signal increases in strength as $\vec{H}$ is tilted from ⟨0001⟩ and is strongest over most of its angular range for $\vec{E}_{rf}$ parallel to $\vec{H}$. We attribute the absence of a CR signal from the orbit around the outside of the waist to the fact that this orbit is sharply cusped [see Fig. 8(b) of Ref. 3] with only a small portion of the orbit in the skin depth, and to magnetic breakdown which couples the orbit to the cigar-shaped electron surface in the third band. Stark has failed to observe a DHVA signal from this orbit while detecting strong signals from breakdown orbits which involve this region of the monster. Thus, the probability of electrons undergoing the six Bragg reflections necessary to execute this orbit is small unless the magnetic field is weak. A value for the cyclotron mass of this orbit for $\vec{H}$ parallel to ⟨0001⟩ can be obtained by taking three times the mass of Stark's A orbit and subtracting four times the mass of the central orbit on the third-band cigar. The result, $m^*/m_0 = 1.25 \pm 0.07$, is significantly less than the value of 1.37 ± 0.02 which we obtain from the r signal for the same direction of $\vec{H}$. This further confirms that branch r cannot be assigned to the orbit around the outside of the monster waist.

Branch s is assigned to the orbit around the monster waist, the β orbit of Fig. 1(a). In agreement with this assignment, the s signal has a minimum m^* line shape (see Fig. 3) and is not tilt sensitive. The s'' branch, which is tilt sensitive, is observed out to 4° from $\langle 11\bar{2}0\rangle$ in the $\{0001\}$ plane. The cutoff angle for this branch is determined by the radius of the inside of the monster waist and the dimensions of the diagonal arm. The pseudopotential FS model yields a value of approximately 6° for this angle, which is consistent with our observations. We have not been able to observe the s branch in specimens with either $\{10\bar{1}0\}$ or $\{11\bar{2}0\}$ surfaces. For these specimens a weak s signal would be obscured by the strong subharmonics of the signal from branch a. We expect the s signal to be weak in $\{10\bar{1}0\}$ and $\{11\bar{2}0\}$ specimens since the portion of the real-space β orbit which lies in the skin depth corresponds to that part of the $\vec{k}$-space orbit which passes over the sharply curved top (or bottom) of the monster waist.[16] Stark has observed DHVA signals from the β orbit with $\vec{H}$ in all three principal crystal planes. The DHVA and CR mass values for this orbit are in excellent agreement (see Table I).

C. Third-Band Lens

Branch a is assigned to the central orbit on the third-band lens [Fig. 1(d)]. The most striking feature of the a signal is the wide variation in its strength between different crystal planes and for different direction of $\vec{H}$ parallel to a given crystal plane. It is the strongest of all the CR signals in Mg when $\vec{H}$ is near the basal plane and the specimen surface is either a $\{10\bar{1}0\}$ or $\{11\bar{2}0\}$ plane. However, it becomes very weak as $\vec{H}$ approaches ⟨0001⟩ and could not be followed unambiguously to ⟨0001⟩ in either of these planes. Furthermore, the a signal could not be detected in specimens with $\{0001\}$ surfaces. These observations give graphic confirmation of the magnetoacoustic re-

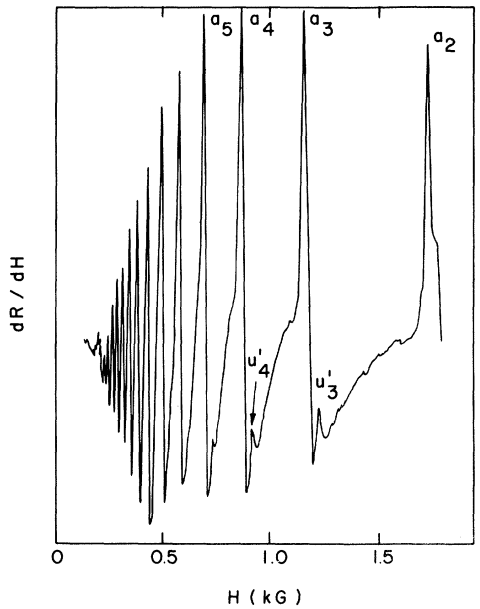

FIG. 6. CR signals in Mg for $\vec{H}$ parallel to $\langle 11\bar{2}0\rangle$ in a $\{10\bar{1}0\}$ surface. $\vec{E}_{rf}$ is perpendicular to $\vec{H}$.

sults which show that the lens is sharply cusped with a radius of curvature over its edge which is only about $\frac{1}{100}$ that of the spherical caps of the lens.

The a signal is not tilt sensitive and over most of its range has the line shape shown in Fig. 3, which agrees well with Chambers's prediction for m^* versus k_H a local maximum. For $\vec{H}$ near the basal plane the line shape of the a signal, shown in Fig. 6, is quite different from any of Chambers's theoretical line shapes. This is not unexpected, since Chambers's analysis assumes that the resonance does not cause an appreciable change in the surface impedance,[7,17] an assumption which is very likely violated because of the large number of electrons which contribute to the lens signal when $\vec{H}$ is near the basal plane.

Figure 7 shows the cyclotron resonance signal for $\vec{H}$ parallel to $\langle 0001\rangle$ in the $\{10\bar{1}0\}$ plane and $\vec{E}_{rf}$ perpendicular to $\vec{H}$. At approximately 11 kG we see what appear to be the fundamentals of three weak closely spaced resonance series with identifiable second and third subharmonics at the appropriate field strengths. As indicated in Fig. 7, the central signal is that of branch r of the mass plot. The peak on the high-field side of the r signal, which yields an m^*/m_0 of about 1.39, was observable only for $\vec{H}$ within approximately 0.5° of $\langle 0001\rangle$. This signal may arise from the central orbit on the lens, though such an assignment is very tentative. The m^*/m_0 value for this signal agrees well with Stark's value of 1.40 ± 0.05 for the "giant" orbit in Mg. However, we have rejected this assignment for two reasons. First, if we could see the giant orbit, we should be able to follow it out to about 4° from $\langle 0001\rangle$. Second, Stark's DHVA data show that at 11 kG there is still an appreciable probability of Bragg reflection at the energy gap which an electron must tunnel

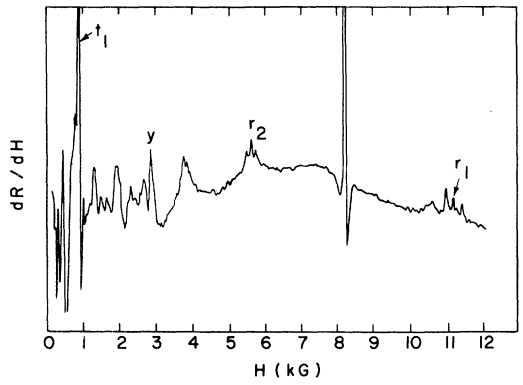

FIG. 7. CR signals in Mg for $\vec{H}$ parallel to $\langle 0001\rangle$ in a $\{10\bar{1}0\}$ surface. $\vec{E}_{rf}$ is perpendicular to $\vec{H}$. The strong signal at 8.2 kG is from a speck of diphenyl pecryl hydrazyl placed in the resonant cavity.

12 times in order to complete the giant orbit. We have seen no other signals involving orbits in the intermediate stage of magnetic breakdown, and do not expect to see such signals. In particular, the fact that the subharmonics of the $m^*/m_0 = 1.39$ signal have strengths comparable to that of the fundamental is inconsistent with the assignment of this signal to the giant orbit. Stark has followed the DHVA signal from the lens all the way to $\langle 0001\rangle$. Unfortunately, near $\langle 0001\rangle$ the signal was too weak to yield reliable mass values. The CR and DHVA masses for $\vec{H}$ in the basal plane are in excellent agreement (see Table I).

The branch b signal is shown in Fig. 5. It is enhanced by tipping $\vec{H}$ from the specimen surface and has the "mass-doubled" inverted line-shape characteristic of a signal from charge carriers on spherical limiting points.[9,18] This signal unquestionably arises from limiting point orbits on the spherical caps of the lens. The mechanism by which it is produced is discussed fully in Refs. 5, 9, and 18. Shaw *et al.*[6] have proposed that the ratio of the angular range over which the limiting point signal from the lens could be observed to the angle subtended by the single-OPW lens could be used as a measure of the degree to which the actual lens corresponds to the single-OPW lens. This suggestion, which seemed to be supported by the Zn and Cd CR data, is definitely contradicted by a comparison of the angular range of the b signals in Cd and Mg. The relevant ratios, 0.8 for Cd and 0.5 for Mg, would imply that the Cd lens is more free-electron-like than the Mg lens. This is certainly not the case.

For H within 10° of $\langle 0001\rangle$ and $\vec{E}_{rf}$ perpendicular to $\vec{H}$, a weak resonance series is seen with a mass essentially the same as that of branch b. In Fig. 7 this signal can be seen on the low-field side of the r signal. We attribute this signal to electrons which are on lens orbits sufficiently removed from the limiting point to have appreciable components of velocity perpendicular to $\vec{H}$. The corresponding signals in Zn and Cd have been assigned to branch j of the Zn and Cd mass plots. The reader should consult Refs. 6 and 9 for a discussion of why one can see CR signals from such orbits, even though $\partial m^*/\partial k_H$ is not strictly zero.

D. Third-Band Cigar

Branch t is assigned to the central orbit on the third-band cigar [Fig. 1(c)]. The maximum m^* line shape and lack of tilt sensitivity exhibited by this signal over most of its angular range agree well with this assignment. The t signal is very strong for $\vec{H}$ near $\langle 0001\rangle$ in a $\{10\bar{1}0\}$ plane, but completely absent from the $\{11\bar{2}0\}$-plane data.

This confirms Stark's conclusion, based on his DHVA data and pseudopotential calculation, that the corners of the cigar are only slightly rounded by the very weak $\langle 10\bar{1}0\rangle$ energy gap. As $\vec{H}$ approaches $\langle 11\bar{2}0\rangle$ the t signal becomes much weaker and broadens. This broadening seems to be the result of a mass spread in the orbits contributing to the resonance since a much narrower signal can be obtained by tilting $\vec{H}$ slightly from the specimen surface. The $\langle 11\bar{2}0\rangle$ mass value recorded in Table I was obtained with $\vec{H}$ tilted 0.1° from the surface.

The strength of the cigar signal for $\vec{H}$ near $\langle 0001\rangle$ would at first appear to contradict our previous comments regarding the absence of CR signals from orbits in the intermediate stage of magnetic breakdown. We conclude either that the probability of magnetic breakdown from the cigar to the monster in the vicinity of the $K\Gamma M$ plane is negligible for field strengths below 1 kG or that the t signal comes from orbits on the cigar which are above and below the region of breakdown.

E. Third-Band Butterflies and Fourth-Band Electron Pockets

The third-band butterflies [Fig. 1(e)] and fourth-band electron pockets [Fig. 1(f)] are separated from one another across the AHL plane by a spin-orbit energy gap which is very small over the entire plane and vanishes along the AL zone line. Neglecting this energy gap leads to a combination sheet which is shaped like a clam [see Fig. 8(f) of Ref. 2]. Stark's DHVA data for $\vec{H}$ near the $\{0001\}$ plane show no evidence of signals from the central orbits on the butterflies or fourth-band electron pockets but contain several signals (the C branches of his area plot) which have been successfully assigned to the clam-shaped combination sheet. Similarly, the CR data indicate that even for field strengths as low as 1 kG the clam-shaped sheet is the appropriate one to use *for orbits which pass near the AL line and lie in planes that are tilted substantially from* $\{0001\}$.

Branch u of the mass plot is assigned to the central orbit on the clam. The line shape of the u signal, shown in Fig. 4, corresponds to m^* versus k_H a local maximum, and the signal is not appreciably affected by tilting $\vec{H}$ slightly from the specimen surface. There is a close correspondence between the various u subbranches and the C branches of Stark's area plot. We attach no significance to the slight discrepancy between the CR and DHVA mass values for this orbit when $\vec{H}$ is parallel to $\langle 1120\rangle$ (see Table I).

For $\vec{H}$ parallel to $\langle 0001\rangle$, only one clam orbit of extremal area is possible. This orbit lies in a plane between the AHL plane and the plane of the self-intersecting clam orbit. It has the shape shown in Fig. 5 of Ref. 1. Branch v of the mass plot is tentatively assigned to this orbit. As $\vec{H}$ is tilted from $\langle 0001\rangle$ in the $\{11\bar{2}0\}$ plane the v branch should split into two branches, one decreasing in mass and the other increasing. We attribute our failure to see the decreasing m^* branch as well as the absence of any v signal in the $\{10\bar{1}0\}$ plane to the fact that the edges of the clam are quite sharp. The signal we do see comes, if our assignment is correct, from the clam which is oriented so that the part of the orbit with the largest radius of curvature lies in the skin depth. The line shape of the v signal corresponds to a broad maximum in m^* versus k_H and the strongest signals were seen in specimen surfaces with an appreciable amount of curvature. The strength of the signal was *enhanced* by tipping $\vec{H}$ from the surface. This enhancement is attributed to reduction of mass spread in the orbits contributing to the resonance. The entries in Table I show good agreement between the CR and DHVA values of m^* for this orbit for $\vec{H}$ parallel to $\langle 0001\rangle$. In fact, it was this agreement which first suggested to us the assignment of the v signal to this orbit.

There are two aspects of the data for the v signal which seem in conflict with the above assignment. The first is the rather slow rate of increase of m^* for the v branch as $\vec{H}$ is rotated from $\langle 0001\rangle$, and the fact that the v branch can be followed out to almost 60° from $\langle 0001\rangle$ where the corresponding v orbit is tilted only a few degrees from the $\{10\bar{1}1\}$ plane, the plane which contains the sharp edge of the clam. The second and more disturbing aspect of the data is that over the entire range of the v branch the signal is seen only with $\vec{E}_{rf}$ perpendicular to $\vec{H}$.

Branch w is assigned to the central orbit on the fourth-band electron pocket [Fig. 1(f)]. With this assignment, w should split into two subbranches as $\vec{H}$ is rotated away from $\langle 0001\rangle$ in both the $\{10\bar{1}0\}$ and $\{11\bar{2}0\}$ planes. Near $\langle 0001\rangle$ the w signal is quite broad, complicated, and tilt sensitive, and is very likely a superposition of signals from these two subbranches. With $\vec{H}$ parallel to $\langle 0001\rangle$ magnetic breakdown between the fourth-band electron pocket and the butterfly [Fig. 1(e)] in the region where the central orbit passes through the AL line of the zone is frustrated by the fact that the electron is moving parallel to the energy gap across the $\{0001\}$ plane. When $\vec{H}$ makes an appreciable angle with $\langle 0001\rangle$, this breakdown occurs (and leads to the clam orbits) *except* for the fourth-band electron pocket which is oriented so that its central orbit passes through the HL line of the zone. It is to this orbit that we attrib-

ute the w signal which we see at all orientations in the $\{11\bar{2}0\}$ plane.

Stark's L_1^1 and L_2^1 DHVA signals correspond to our w signals in the $\{10\bar{1}0\}$ and $\{11\bar{2}0\}$ planes, respectively. He has assigned these signals to central orbits on lens-shaped surfaces which result if there is magnetic breakdown between the fourth-band electron pockets and the butterflies at the $\langle 10\bar{1}0\rangle$ energy gap as well as across the $\{0001\}$ plane. Actually, there is no real conflict between our data and Stark's since for $\vec{H}$ near $\langle 0001\rangle$ the L_1^1 orbit is essentially identical to that on the corresponding electron pocket, and the L_2^1 orbit and that on the corresponding electron pocket are identical over the entire $\{11\bar{2}0\}$ plane. The m^*/m_0 of our $\{11\bar{2}0\}$ w signal has a minimum value of 0.30 $\pm$ 0.01 for $\vec{H}$ approximately 28° from $\langle 0001\rangle$. This agrees with Stark's L_2^1 data, which give a minimum m^*/m_0 of 0.32 $\pm$ 0.01 for $\vec{H}$ 26.8° from $\langle 0001\rangle$. Similarly, the CR and DHVA mass values for this orbit are in good agreement for $\vec{H}$ parallel to $\langle 0001\rangle$ (see Table I). Consistent with our interpretation of the w branch is the fact that the w signal has a maximum m^* line shape and is not tilt sensitive over most of its angular range.

Stark explains his failure to follow any of his L branches beyond 45° from $\langle 0001\rangle$ to fairly rapid growth of the $\langle 10\bar{1}0\rangle$ energy gap as one goes out of the AHL plane. This cannot be responsible for the loss of the L_2^1 or L_2^4 branches, since the orbits to which these signals have been assigned are always centered on the HL line of the zone.

Given the above assignment of the w branch, the x branch must be assigned to the third-band butterfly central orbit which passes through the HL line of the zone. The w and x branches coincide to within experimental error for $\vec{H}$ parallel to $\langle 10\bar{1}0\rangle$. The fact that for $\vec{H}$ near $\langle 10\bar{1}0\rangle$ both these signals are seen only with $\vec{E}_{rf}$ parallel to $\vec{H}$ indicates that the $\langle 10\bar{1}0\rangle$ energy gap causes little rounding of the fourth-band electron pockets or the butterflies. This conclusion agrees with the sharp $\{10\bar{1}0\}$ plane edges of these surfaces predicted by the pseudopotential band-structure calculation (see Fig. 7 of Ref 3). The lack of tilt sensitivity of the x signal agrees with our orbit assignment. Our failure to see the w or x branches for $\vec{H}$ near $\langle 10\bar{1}0\rangle$ in $\{0001\}$ specimens is readily explained by the short time that electrons on these orbits spend in the skin depth when the specimen surface is an $\{0001\}$ plane. The one feature of the x signal which seems at odds with our orbit assignsignment is its line shape, which resembles that of a maximum in m^* versus k_H. Also disturbing is our failure to see a signal from the central orbit on the butterfly for $\vec{H}$ near $\langle 0001\rangle$. However, as previously mentioned, the w signal for $\vec{H}$ near $\langle 0001\rangle$ is quite broad. It may well contain a butterfly orbit signal buried within it. Stark has not reported any DHVA signals for $\vec{H}$ near $\langle 10\bar{1}0\rangle$ that correspond to our w or x branches.

F. Magnetic Breakdown Orbit

The signal associated with branch y appears as a single resonance line for $\vec{H}$ in the $\{10\bar{1}0\}$ plane (see Fig. 7). In the $\{11\bar{2}0\}$ plane several subharmonics are observed, but are very narrow and appreciably smaller in amplitude than the fundamental. For $\vec{H}$ parallel to $\langle 0001\rangle$, m^* for the y branch is almost exactly three times that for branch d, which has been assigned to orbits on the diagonal arms of the monster [the γ orbit of Fig. 1(a)]. The y branch is assigned to a trifoliate-shaped orbit which results from magnetic breakdown between the third-band cigar and the diagonal arms of the monster (see Fig. 9 of Ref. 2). A DHVA signal from this orbit has been observed by Stark, and the DHVA and CR masses are in good agreement (see Table I). Our simultaneous observation of the diagonal arm orbit and the breakdown orbit seems a contradiction of our contention that we do not see orbits in the intermediate stage of magnetic breakdown. We conclude that the orbits responsible for the d and y signals must occur at different heights above the $K\Gamma M$ plane.

V. CONCLUSIONS

The results of this investigation are in excellent agreement with the detailed structure of the FS of Mg determined by Stark and his co-workers. The absence of CR signals from the "giant" orbit and the hexagonal grid of coupled orbits so prominent in the DHVA data confirms Moore's[10] conclusion that CR signals will not be seen from orbits in the intermediate stage of magnetic breakdown. Where DHVA and CR masses are both available for the same orbit, the mass values are in good agreement.

ACKNOWLEDGMENTS

The authors would like to thank W. L. Gordon for many helpful discussions on all aspects of this work and R. E. Powell for taking some of the data and growing some of the Mg crystals. One of us (D.A.Z.) is grateful to NASA for the grant of a Graduate Fellowship under the tenure of which this work was carried out. We are especially indebted to R. W. Stark for instruction in the art of producing high-purity Mg crystals and for informing us of the results of his work prior to publication.

*Work supported in part by the U.S. Air Force Office of Scientific Research under Grant Nos. AF-AFOSR-536-66 and 69-1637.

†Present address: Department of Physics, Ohio State University, Columbus, Ohio.

[1]J. B. Ketterson and R. W. Stark, Phys. Rev. 156, 748 (1967).

[2]R. W. Stark, Phys. Rev. 162, 589 (1967).

[3]J. C. Kimball, R. W. Stark, and F. M. Mueller, Phys. Rev. 162, 600 (1967).

[4]T. G. Eck and M. P. Shaw, in *Proceedings of the Ninth International Conference on Low-Temperature Physics, Columbus, Ohio*, edited by J. G. Daunt *et al.* (Plenum, New York, 1965), p. 759.

[5]M. P. Shaw, P. I. Sampath, and T. G. Eck, Phys. Rev. 142, 399 (1966).

[6]M. P. Shaw, T. G. Eck, and D. A. Zych, Phys. Rev. 142, 406 (1966).

[7]R. G. Chambers, Proc. Phys. Soc. (London) 86, 305 (1965).

[8]W. A. Harrison, Phys. Rev. 118, 1190 (1960).

[9]F. W. Spong and A. F. Kip, Phys. Rev. 137, A431 (1965).

[10]T. W. Moore, Phys. Rev. Letters 18, 310 (1967).

[11]R. W. Stark (unpublished).

[12]For further details see D. A. Zych, Ph.D. thesis, Case Institute of Technology, 1967 (unpublished).

[13]J. F. Koch, R. A. Stradling, and A. F. Kip, Phys. Rev. 133, A240 (1964).

[14]R. E. Powell and T. G. Eck (unpublished).

[15]R. W. Stark, T. G. Eck, and W. L. Gordon, Phys. Rev. 133, A443 (1964).

[16]Note that the projection of the real-space orbit on a plane perpendicular to $\vec{H}$ has the same shape as the $\vec{k}$-space orbit but is rotated about $\vec{H}$ by 90°.

[17]T. W. Moore, Phys. Rev. Letters 16, 581 (1966).

[18]C. C. Grimes, A. F. Kip, F. Spong, R. A. Stradling, and P. Pincus, Phys. Rev. Letters 11, 455 (1963).

PHYSICAL REVIEW B VOLUME 1, NUMBER 12 15 JUNE 1970

Gravitation-Induced Electric Field near a Metal. II *

L. I. Schiff

Institute of Theoretical Physics, Department of Physics, Stanford University, Stanford, California 94305
and Theoretical Physics Group, Imperial College, London S.W.7, England

(Received 15 December 1969)

It is shown that screening of the ionic lattice by conduction electrons is insufficient to account for the zero acceleration found in the experiment of Witteborn and Fairbank on the free fall of electrons within a metallic shield. A speculative suggestion is made for reconciling this conclusion with the results of the centrifuge experiment of Beams and the uniform-compression experiment of Craig.

I. HISTORICAL INTRODUCTION

The matters under discussion in this paper first arose in connection with proposed experiments on the free fall of electrons and positrons.[1] In order that the extremely weak force exerted by the earth's gravitational field on an electron be measurable, it is necessary that the electron be shielded from stray electric fields. This is accomplished by enclosing the experimental region in a vertical metal tube of circular cross section. However, it was suggested at an early stage[2] that earth gravity, acting on the metal, might produce an electric field within the tube which would complicate the interpretation of the experiment. A detailed quantum-mechanical calculation was then performed[3] which concluded that the gravitation-induced electric field within the tube is expected to be $-(mg/e)\hat{z}$, where m and $-e$ are the mass and charge of an electron, g is the acceleration of gravity, and $\hat{z}$ is a unit vector in the upward direction. This field just cancels the downward gravitational force on a free electron and doubles the downward gravitational force on a free positron.[4] The experiment, performed by Witteborn and Fairbank,[5] confirms this prediction for electrons. The measured acceleration is zero with an uncertainty of $\pm 0.09g$.

A different view of the theoretical situation was then presented by Dessler, Michel, Rorschach, and Trammell,[6] who argued that the differential compression of the ionic lattice would lead to an electric field roughly ten thousand times larger and in the opposite direction, a field of order $+(Mg/e)\hat{z}$, where M is the ionic mass. On the other hand, lattice compression effects were estimated to be negligible both in the original theoretical paper[3] and in a subsequent investigation.[7]

Herring[8] resolved this theoretical disagreement by showing how the reciprocity-relation approach